Title

Reactions of Molten LiI with I2, H2O, and O2 Relevant to Halogen-Mediated Oxidative Dehydrogenation of Alkanes

Journal

The Journal of Physical Chemistry C, 120(9)

ISSN

1932-7447

Authors

Huang, Chang
Kristoffersen, Henrik H
Gong, Xue-Qing
et al.

Publication Date

2016-03-10

DOI

10.1021/acs.jpcc.5b12336

Reactions of Molten LiI with I_2, H_2O, and O_2 Relevant to Halogen-Mediated Oxidative Dehydrogenation of Alkanes

Chang Huang[†,‡], Henrik H. Kristoffersen[†], Xue-Qing Gong[‡], and Horia Metiu*[,†]

[†]Department of Chemistry and Biochemistry, University of California, Santa Barbara, California 93106-9510, United States

[‡]Key Laboratory for Advanced Materials, Centre for Computational Chemistry and Research Institute of Industrial Catalysis, East China University of Science & Technology, Meilong Road 130, Shanghai 200237, China

*805-893-2256, metiu@chem.ucsb.edu

Abstract

Constant-temperature *ab initio* molecular dynamics is used to study reactions between molten LiI and gas phase molecules (O_2, H_2O, and I_2) in an attempt to elucidate some aspects of the alkane oxidative dehydrogenation activity performed in the presence of molten LiI. We investigate the energy of reactions that produce LiIO, $LiIO_3$, $LiIO_4$, Li_2O_2, Li_2O, LiOH, and I_2. We find that the most favorable process is the formation of gaseous I_2, co-produced with LiOH or Li_2O (depending on the availability of water). If water is absent, some $LiIO_4$ will also be formed. However, this is unlikely to happen during oxidative dehydrogenation, because LiI is very hydroscopic and the oxidative dehydrogenation reaction produces water.

1. Introduction

Alkenes (ethylene, propylene, styrene, etc.) are basic compounds in industrial organic chemistry. Currently they are obtained by thermal dehydrogenation of ethane, propane or ethylbenzene.[1-3] These reactions are equilibrium-limited, require high temperature, use large amounts of energy, and are plagued by catalyst coking. Many approaches have been proposed for overcoming these difficulties. One of the most popular is oxidative dehydrogenation (ODH), where the endothermic dehydrogenation of alkanes is combined with the exothermic formation of water from O_2 and hydrogen. In spite of much effort, no commercially successful ODH catalyst has been found.[4-5] An alternative is halogen-mediated ODH (HM-ODH) which is formally described by the following reactions:

$$R\text{-}CH_2CH_3 + X_2 \rightarrow R\text{-}CH{=}CH_3 + 2HX \quad (1)$$

$$2HX + \tfrac{1}{2}\, O_2 \rightarrow X_2 + H_2O \quad (2)$$

The sum of these reactions is

$$R\text{-}CH_2CH_3 + \tfrac{1}{2}\, O_2 \rightarrow R\text{-}CH{=}CH_3 + H_2O \quad (3)$$

which is the ODH reaction. This scheme has been carried out by exposing a mixture of hydrocarbon and oxygen to molten LiI.[6-9] LiI is utilized as an I_2 source through the reaction $2LiI + \tfrac{1}{2}O_2 \rightarrow I_2 + Li_2O$.[10] If the hydrocarbon was propane, the propylene yield was around 60 %, which is competitive with the existing industrial dehydrogenation processes. HM-ODH has several advantages when compared to the existing industrial dehydrogenation: it is exothermic (the industrial dehydrogenation is very endothermic), it

does not require vacuum or the dilution of the feed with steam, it is carried out at lower temperatures, and coking is not a problem. The molten salt has high heat capacity and heat conductivity and hot-spot formation is less likely. A substantial disadvantage is that molten LiI, LiOH, and the mixture of HI and water are very corrosive.

The experimental results do not make clear the role of the molten LiI salt. It is possible that LiI is only a source of I_2 and the HM-ODH reactions take place in the gas phase, but it is also conceivable that some chemistry takes place at the surface of the molten salt. This may happen if the oxygen reacts with the salt and makes oxygen containing iodine compounds which then oxidize the alkane. Another possibility is that I_2 dissolves in the molten salt and this dissolved form reacts with the alkanes.

In this paper, we use *ab initio*, constant-temperature, molecular dynamics to investigate the solvation of H_2O, I_2, and O_2 in molten LiI and the reaction of gaseous O_2 with molten LiI. It is found that, at 800K, it is thermodynamically preferable that dry O_2 gas reacts with the molten LiI to produce I_2, solid Li_2O (Li_2O is not soluble in LiI) and a minor amount of $LiIO_4$. In the presence of water, the reaction of O_2 with molten LiI produces only LiOH and I_2. LiOH is soluble in molten LiI. The calculations suggest that the main oxidant in alkane dehydrogenation is I_2, which can exist as either gaseous I_2 or as I_4^{2-} ions dissolved in the salt.

2. Computational methods

The catalyst is modeled by a thin film of molten LiI (40 LiI units) in a periodic 12.6Å×12.6Å×44.0Å supercell. The LiI film is free standing and has a thickness of about

25Å. *Ab-initio*, constant temperature molecular dynamics (MD) simulations are carried out using the VASP program.[11-14] The energies and the forces acting on the atoms are calculated with density functional theory (DFT) and the PBE functional.[15] A plane-wave basis set with a 350 eV energy cut-off is used and all calculations are performed at the Γ-point. The valence electrons (one for H and Li, six for O, and seven for I) are treated with the PAW method and the core electrons are treated with the frozen core approximation. To assess the importance of spin, both spin-polarized and spin-paired calculations have been performed. It was found that the spin-paired electronic structure is correct (lowest energy), when the system does not contain O_2 molecules. With one O_2 molecule, the system is a triplet. We therefore impose a triplet spin electronic structure in MD simulations that contain an O_2 molecule, but we do not use spin-polarized calculations for the other simulations. We are aware that spin-orbit coupling and van der Waals interactions are not properly accounted for in this study. However, we calculate energy differences and therefore some of these effects are cancelled. Furthermore the conclusions reached are based on energy difference of the order of 1 eV and therefore it is unlikely that they will be changed by inclusion of van der Waals interactions or spin-orbit coupling.

The MD simulations are performed at constant N, V, T (particle number, volume and temperature, respectively) with a Nosé thermostat that keeps the temperature around 800K.[16] The Born-Oppenheimer approximation is used, which is accurate due to the large band gap in the system. The atomic motions are treated classically and propagated with 1-femtosecond time steps. The internal energy of different systems is obtained from the MD simulations as the time average kinetic and potential energy:

$$\langle E \rangle_t = \frac{1}{t - t_0} \int_{t_0}^{t} K(t') + U(t') \; dt' \tag{4}$$

The time t_0 is chosen to allow the system to equilibrate and lose memory of the initial conditions; it was found that between 0.3 and 3.4 picoseconds were sufficient for this purpose. The only exception is the solvation of I_2 for which t_0= 10.3 picoseconds; this was necessary because I_2 combines with two I^- ions over a 10 ps timespan. The MD simulations are subsequently sampled for at least 9 ps ($t - t_0 \geq 9$ ps). Solvation and reaction energies are obtained by subtracting the mean energy of the initial state from the mean energy of the final state. In this way, the solvation energy of a molecule is calculated as the mean energy of the solvated molecule in LiI(*l*), minus the mean energy of pure LiI(*l*), minus the mean energy of the molecule in the gas phase. We add $\frac{3}{2} k_B T$ to internal energies of gas phase molecules, because VASP fixes the center of mass for these MD simulations, so translational kinetic energy is not included.

The limitation in computational resources necessitates relatively short molecular dynamics simulations. Therefore, it is possible that the molten LiI system gets trapped in some local minimum or that it retains memory of the starting configuration. Such issues may result in errors in the time average energies. However, the main conclusions regarding which molecular species are soluble in molten LiI and which reaction products are energetically favorable are based on energy differences that are larger than the possible errors in the calculations.

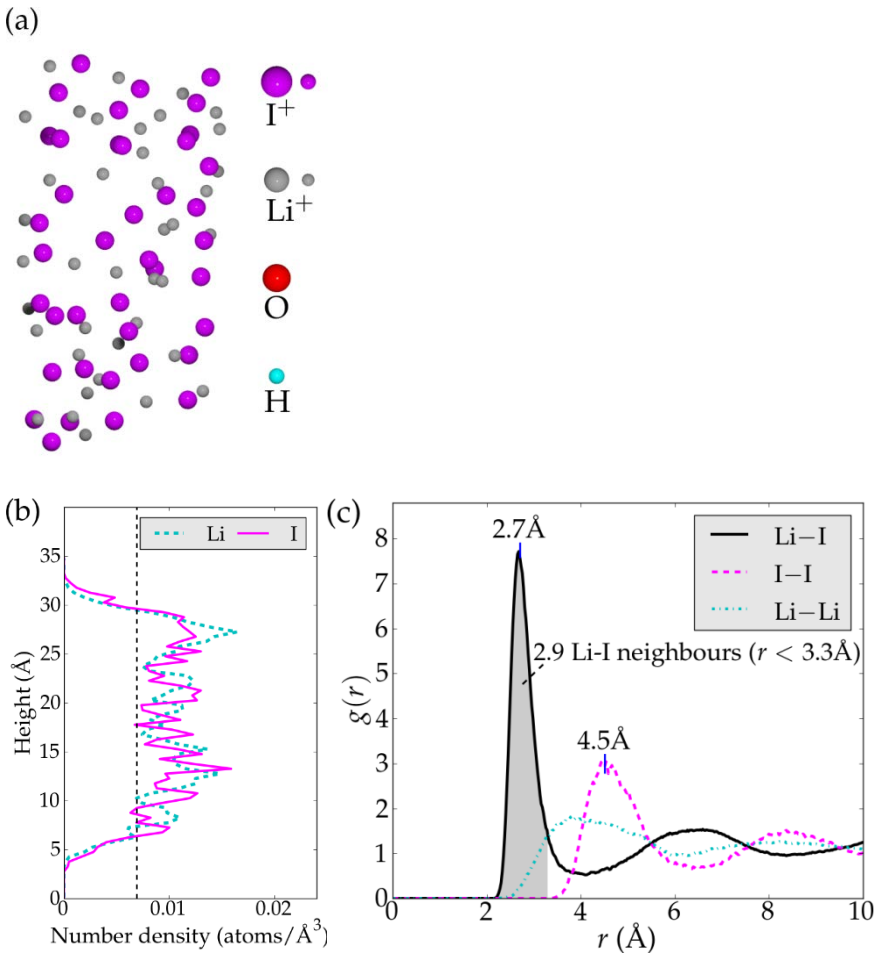

Figure 1. (a) Side view of the pure LiI(*l*) film at the end of the 14-ps MD simulation. (b) Number density of Li and I atoms in the film as a function of height in the computational cell. The vertical dashed line marks the experimental number density for Li and I in molten LiI at 800 K.[17] (c) Radial pair-distribution functions $g_{\mathrm{Li–I}}(r)$, $g_{\mathrm{Li–Li}}(r)$, and $g_{\mathrm{I–I}}(r)$. The function $g_{\mathrm{A–B}}(r)$ is defined such that $p_{\mathrm{A–B}}\,\mathrm{d}r = 4\pi\, r^2\, g_{\mathrm{A–B}}(r)\, \rho_{\mathrm{B}}\,\mathrm{d}r$, where $p_{\mathrm{A–B}}(\mathrm{r})\,\mathrm{d}r$ is the probability of finding an atom B at a distance between r and $r + \mathrm{d}r$ from A and ρ_{B} is the number density of atom B calculated by estimating the volume of the film to be $12.6 \times 12.6 \times 25$ Å^3.

3. Structure of the molten LiI film

In this section we discuss the structural properties of the pure LiI(*l*) thin film obtained from a 14-ps MD simulation. Figure 1(a) shows a side view of the atomic configuration at the end of the MD simulation and the Supporting Information contains a movie of the MD simulation. The purpose of the movie is to demonstrate that the ions change their position and sample a variety of configurations. The LiI(*l*) thin film is therefore a liquid and not an amorphous solid.

Figure 1(b) shows the time-averaged number density of I and Li atoms in the film as a function of position perpendicular to the film surface. This was calculated by averaging in time over the number of atoms (ions) between two planes parallel to the surface of the liquid film, and separated by 0.5 Å. We find no segregation of the Li^+ and I^- ions at the molten salt–vacuum interfaces. Such segregation has been observed in aqueous electrolyte solutions,[18] but it is less likely in this system because of the large ion concentration and the constraints imposed by charge neutrality. The average atomic density of both Li and I in the bulk is found to be higher than expected from the experimental density of bulk molten LiI (black dashed line).[17] This may be caused by the fact that the film is thin.

The radial pair-distribution functions ($g(r)$) for Li−I, Li−Li, and I−I are shown in Figure 1(c). The average Li−I bond length (2.7 Å) and Li−Li / I−I bond length (~4.5 Å) is in reasonable agreement with the 2.85 Å and 4.45 Å found by X-ray diffraction messurements.[19] By integrating the probability of finding an atom of the opposite type in the first peak of the Li−I radial pair-distribution function, we find that the average number of Li−I neighbors is 2.9 (r < 3.3 Å). This is less than the 5.6 neighbors obtained

in the X-ray diffraction experiment. Some of the discrepancy is due to the atoms situated at the molten salt–vacuum interfaces, which inevitably have lower number of neighbors, but it does not explain all of the difference. It is not easy to reconcile the observations of too high bulk density, accurate bond lengths, and too few nearest neighbor atoms at the same time.

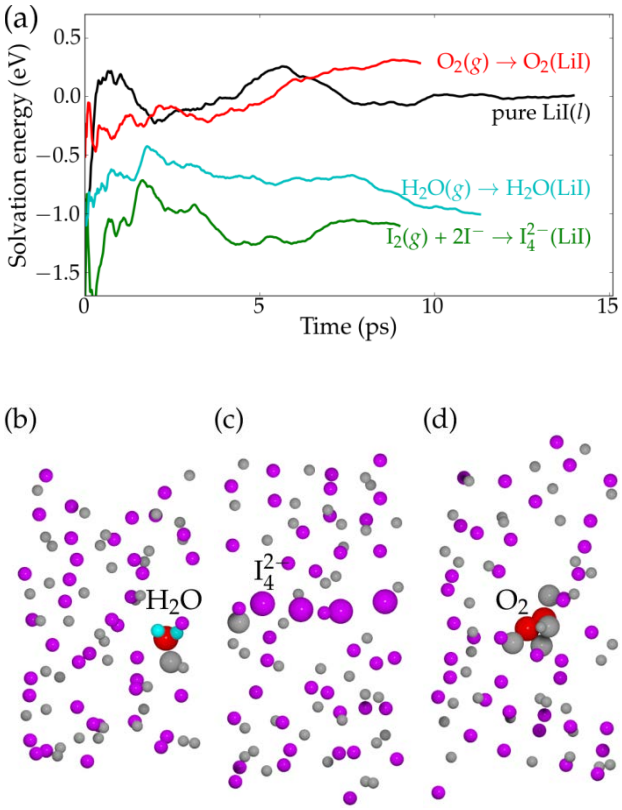

Figure 2. (a) Mean solvation energies as a function of elapsed time ($t-t_0$) for H_2O, I_2, and O_2 solvated in LiI and compared to the molecules in the gas phase and pure LiI(l) (0 eV). Final atomic configuration in the MD sampling for (b) solvated H_2O, (c) solvated I_2 (exist

as an I_4^{2-} species) and (d) solvated O_2. Li atoms closer than 2.5 Å from the solvated species have increased radii.

4. Solvation of H_2O, I_2 and O_2 in molten LiI

LiI, like most other molten alkali halides, is very hygroscopic[20] and the ODH reaction (3) produces water. For these reasons we examine water solvation by placing a water molecule inside the molten LiI film, performing a MD simulation of this system to obtain the internal energy, and subtracting the internal energy of the pure LiI thin film and that of gaseous H_2O. We find that there is a mean energy gain of –1.0 eV when the water molecule is dissolved in the salt (Figure 2(a)). Figure 2(b) shows that the O atom of the water molecule interacts with a Li^+ cation (the O-Li distance is less than 2.5 Å). Such interactions are present throughout the MD simulation with the water molecule "jumping" from one Li^+ cation to another Li^+ cation by coordinating to two Li^+ cation for short period of time. The solvation of H_2O in LiI(*l*) is found to be more favorable than solvation in LiCl(*l*) supported on MgO(*s*), which results in an energy gain of –0.6 to –0.7 eV.[21] This is likely because the electrostatic interaction of Li^+ with I^- is weaker than the interaction of Li^+ with Cl^-, so the Li^+ cations are more free to bind to water. The Supporting Information includes a movie of the MD simulation for solvated H_2O in LiI(*l*).

Next we investigate solvation of an I_2 molecule in the molten LiI. Gaseous I_2 formation was observed in the ODH experiments, when oxygen gas was passed through the molten LiI.[6-9] The formed I_2 molecules may react with alkanes to produce alkenes and HI,[22] but I_2 could also dissolve in the LiI molten salt. I_2 solvation is found to be energetically favorable with a mean energy stabilization of –1.1 eV (see the green curve

in Figure 2(a)). This indicates that a significant portion of the I_2 molecules produced by the oxidation of molten LiI (in the HM-ODH process) will be dissolved in the molten LiI. The MD simulation of I_2 solvation required a long initial thermalization time (t_0 = 10.3 ps), because I_2 solvation is followed by bond formation between I_2 and two I^- ions. Stable mean energies were only obtained after this process was completed. The linear I_4^{2-} species (shown by four larger purple spheres in Fig. 2(c)), formed through the reaction $I_2(g) + 2I^- \rightarrow I_4^{2-}$, is stable. Linear I_4^{2-} ions are known from compounds such as $[Cu(NH_3)_4]^{2+}I_4^{2-}$.[23] Larger polyions are also possible[24] but they cannot be formed in our simulation because they would exceed the size of the computational cell. The behavior of I_2 dissolved in molten LiI differs from that observed in aqueous LiI solution where I_3^- is the common ion found in connection with I_2 solvation.[25] The I_4^{2-} species spans the entire supercell and one might think that the simulated system forms a long chain consisting of I_4^{2-} units. We argue that this is not the case, because the four I atoms in I_4^{2-} are not equivalent. The average distance between the outer I atom (in I_4^{2-}) and its periodic replica is slightly longer than the internal bond distances in the I_4^{2-} ion (3.34±0.27 Å compared to 3.24±0.25 Å, 3.20±0.26 Å, and 3.24±0.27 Å (±one standard deviation)). These distances are shorter than the average I-I distance (4.5 Å) in pure LiI(*l*) obtained from the radial pair-distribution function (Figure 1(c)) indicating that none of the I atoms are I^- ions any longer. Bader charge analysis was performed on ten configurations separated by 1 ps and selected from the last 9 ps of the simulation. The average Bader charges (± one standard deviation) on the I atoms forming the I_4^{2-} ion are -0.53±0.09 *e*, -0.34±0.08 *e*, -0.37±0.10 *e* and -0.55±0.09 *e*, confirming that the four I atoms are not equivalent. These values are significantly different from the average values

for the surrounding I^- ions (–0.87±0.01 *e*) and Li^+ ions (0.87±0.01 *e*). We conclude that the species I_4^{2-} is formed when I_2 dissolves in molten LiI, but we cannot rule out the possibility that polyions containing more iodine atoms are more stable.

Finally, we investigate O_2 solubility by placing one O_2 molecule in the LiI(*l*) film and fixing the total spin of the system to a triplet state. Solvation is energetically unfavorable: placing O_2 in the liquid increases the average energy by +0.3 eV (Figure 2(a)). Therefore, molecular oxygen is not stabilized in the LiI(*l*) system. The average O−O bond length for O_2 in LiI(*l*) is 1.39±0.10 Å, which is somewhat longer than the average bond length found in the O_2-gas MD simulation (1.24±0.05 Å). This indicates that some electron charge from I^- ions is transferred to the solvated O_2 molecule. The atomic configuration at the end of the MD simulation (Figure 2(d)) supports this, because the O_2 molecule is mainly surrounded by Li^+ ions. However, this interaction is not strong enough to favor the dissolution of O_2.

5. Reactions between O_2 and molten LiI

In this section we investigate possible reactions between O_2 molecules and the LiI system (Eqs 5-10) to form LiIO, $LiIO_3$, and $LiIO_4$ species in the molten salt (Figure 3), as well as the formation of gaseous I_2 together with Li_2O_2, Li_2O, or LiOH species in the molten salt (Figure 4). All of these reactions produce possible oxidizing specie, and the analysis of the energies of these reactions may give information about the possible ODH mechanism.

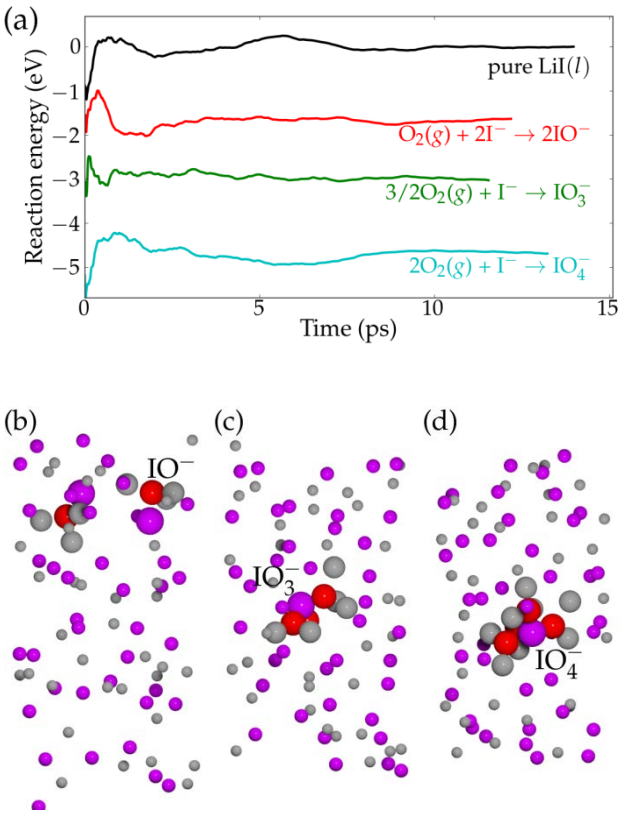

Figure 3. (a) Mean reaction energies as a function of elapsed time ($t–t_0$) for the formation of $2IO^-$ (Eq 5), IO_3^- (Eq 6) and IO_4^- (Eq 7). The internal energy of pure LiI(*l*) is included as it is used as a reference (0 eV). Final configuration in the MD sampling for (b) the two IO^- ions, (c) the IO_3^- ion and (d) the IO_4^- ion. Li atoms closer than 2.5 Å from the product ions have increased radii.

5.1. Formation of oxyanions species. Oxygen and iodine can form a series of oxyanions ($I_xO_y^{z-}$),[26] where most of them are good oxidizing agents.[27-28] First, we consider lithium hypoiodite (LiIO) formed by the reaction

$$O_2(g) + 2I^- \rightarrow 2IO^- \qquad (5)$$

To calculate the energy of this reaction we place two O atoms into the LiI molten salt and calculate the mean energy. To obtain the reaction energy we subtract from this the mean energy of pure LiI(*l*) and that of O_2(*g*). The reaction energy obtained in this way is –1.6 eV (Figure 3(a)). During the initialization of the simulation, both O atoms bind to I^- and form two IO^- species (Figure 3(b)). The I and O atoms in the IO^- species stay together for the entire simulation with an average I-O bond length of 2.04±0.10 Å.

Similarly, the reaction between O_2 and LiI may lead to the formation of lithium iodate ($LiIO_3$)

$$3/2O_2(g) + I^- \rightarrow IO_3^- \quad (6)$$

which is another possible oxyanion. The mean energy of reaction 6 is –3.0 eV (Figure 3(a)). The three I-O bonds in IO_3^- (Figure 3(c)) have average lengths of 1.86±0.07Å, 1.85±0.06Å, and 1.84±0.05Å.

Finally, we put two O_2 into the LiI molten salt system to form lithium periodate ($LiIO_4$) and calculate the mean energy of the reaction

$$2O_2(g) + I^- \rightarrow IO_4^- \quad (7)$$

which is –4.7 eV (Figure 3(a)). The four I-O bonds in IO_4^- (Figure 3(d)) have average lengths of 1.95±0.11 Å,1.88±0.06 Å, 2.02±0.10 Å, and 1.95±0.10 Å.

These results indicate that IO_4^- is energetically the most stable oxyanion, since formation of IO_4^- gives the highest stabilization of the internal energy both per I^- ion consumed and per O_2 molecule consumed ($\Delta E / n_{O_2}$ = –2.4 eV for IO_4^- compared to –1.6 eV for IO^- and –2.0 eV for IO_3^-).

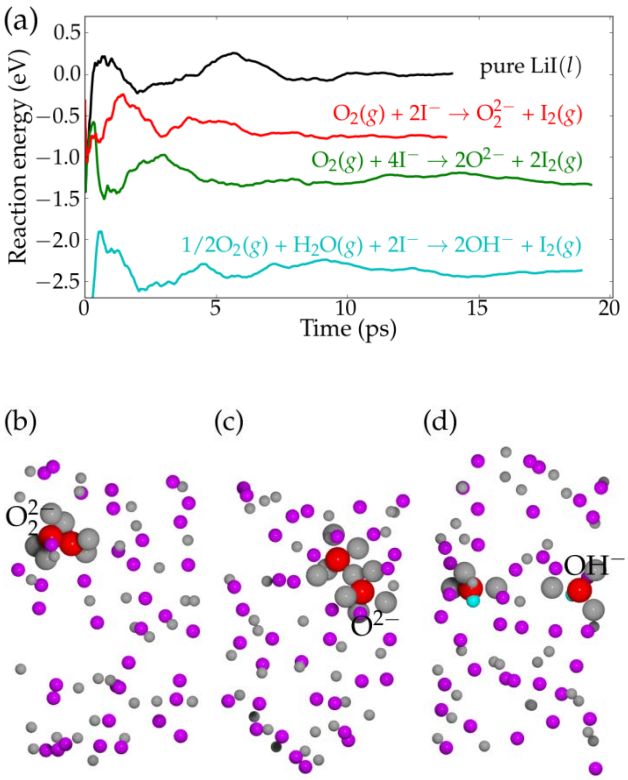

Figure 4. (a) Mean reaction energies as a function of elapsed time ($t-t_0$) for the formation of $O_2^{2-} + I_2(g)$ (Eq 8), $2O^{2-} + 2I_2(g)$ (Eq 9) and $2OH^- + I_2(g)$ (Eq 10). The internal energy of pure LiI(l) is included as it is used as a reference (0 eV). Final configuration in the MD sampling for (b) the O_2^{2-} ion, (c) the two O^{2-} ions and (d) the two OH^- ions. Li atoms closer than 2.5 Å from the product ions have increased radii.

5.2. Formation of I_2 gas and Li_2O_2, Li_2O, or LiOH. An oxygen molecule can also react with LiI to produce I_2 gas and lithium peroxide (Li_2O_2) according to

$$O_2(g) + 2I^- \rightarrow O_2^{2-} + I_2(g) \qquad (8)$$

To calculate the energy of this reaction we insert one O_2 molecule into the molten salt and remove two I atoms to form one I_2 molecule in the gas. By adding the mean energy of

this system to that $I_2(g)$ and subtracting the mean energy of the pure LiI(l) and $O_2(g)$ we find a reaction energy of –0.8 eV (Figure 4(a)). From the MD simulation we observe that O_2^{2-} coordinates to several Li^+ cations (Figure 4b) and that the average O−O bond length is 1.55±0.08Å. This is longer than the bond length we found for solvated molecular O_2 (1.39±0.10 Å) and fits with the bond length in bulk $Li_2O_2(s)$ (1.55 Å).[29] These observations indicate that the oxygen inside the molten salt is a peroxide ion, O_2^{2-}.

Oxygen can also react with the salt to produce $2I_2(g)$ and lithium oxide (Li_2O) (rather than Li_2O_2)

$$O_2(g) + 4I^- \rightarrow 2O^{2-} + 2I_2(g) \quad (9)$$

The mean energy of this reaction is –1.3 eV (Figure 4(a)). The average O−O bond length is 3.42±0.40 Å (±one standard deviation). The large distance indicates that, unlike the case of O_2^{2-}, there is no O−O bond when $2Li_2O$ is formed. A snapshot of the atomic configuration surrounding the two O^{2-} ions shows that each O^{2-} ion binds to five Li^+ with one of the Li^+ binding to both O^{2-} ions (Figure 4(b)). The energy of Eq 9 is more negative than the energy of Eq 8, which indicates that the Li_2O(LiI) is more stable than Li_2O_2(LiI). However, the reaction path to $2O^{2-}$ requires breaking the O−O bond, which may have a high barrier, i.e., slow kinetics.

So far, water has not been part of the reactions considered. However, water is produced in the ODH reaction and our calculations show that water has a high stability in molten LiI. Therefore, we have also studied the reaction

$$½O_2(g) + H_2O(g) + 2I^- \rightarrow 2OH^- + I_2(g) \quad (10)$$

Two I^- ions are exchanged with two OH^- ions to produce LiOH and I_2 gas. The reaction energy is –2.4 eV (Figure 4(a)). A snapshot of the atomic configuration at the end of the MD simulation shows two separate OH^- ions that are each surrounded by three Li^+ ions (Figure 4(d)).

5.3. Thermodynamic stability of the considered species. The mean energy changes associated with the reactions between $O_2(g)$ and LiI(l) are summarized in Table 1. At 800 K, entropy contributes significantly to the reaction Gibbs free energy, and it must be accounted for. Unfortunately, the entropy change is not directly accessible from the MD simulations and has to be estimated separately. Our approach is to use pure phase entropy data, which are available for some species we consider: LiI(l), $O_2(g)$, $H_2O(g)$, $Li_2O(l)$, LiOH(l), and $I_2(g)$ [http://kinetics.nist.gov/janaf/]. Data for $LiIO_4(l)$ are not available and we use the entropy of $2O_2(g) + LiCl(l) \rightarrow LiClO_4(l)$ as a substitute. The entropy change for reactions 7, 9, 10 can be estimated from these pure phase values, and the estimated change in Gibbs free energy is obtained as $\Delta G^{o}_{estimate} = \Delta E + p\Delta V - T\Delta S^{o}_{estimate}$. The volume change ($\Delta V$) is assumed to originate purely from changes in the number of gas phase molecules (Δn_{gas}) and is calculated by the ideal gas law ($p\Delta V = \Delta n_{gas} k_B T$).

Table 1. Energies (ΔE) and estimated free energies ($\Delta G^{o}_{estimate}$) for reactions 5-10

	ΔE	$\Delta G^{o}_{estimate}$
$40LiI(l) + O_2(g) \rightarrow 2LiIO(LiI) + 38LiI(l)$	–1.6 eV	

$40LiI(l) + 3/2O_2(g) \rightarrow LiIO_3(LiI) + 39LiI(l)$	–3.0 eV	
$40LiI(l) + 2O_2(g) \rightarrow LiIO_4(LiI) + 39LiI(l)$	–4.7 eV	–2.5 eV [a]
$40LiI(l) + O_2(g) \rightarrow Li_2O_2(LiI) + I_2(g) + 38LiI(l)$	–0.8 eV	
$40LiI(l) + O_2(g) \rightarrow 2Li_2O(LiI) + 2I_2(g) + 36LiI(l)$	–1.3 eV	–1.1 eV
$40LiI(l) + ½O_2(g) + H_2O(g) \rightarrow 2LiOH(LiI) + I_2(g) + 38LiI(l)$	–2.4 eV	–1.6 eV

[a] Entropy contribution for $LiIO_4$ formation is based on entropy data for $LiCl(l)$, $O_2(g)$ and $LiClO_4(l)$, since data for $LiIO_4(l)$ are not available.

The negative reaction energies and Gibbs free energies indicate that several reactions are possible and that there will be a competition between formations of the different products. The abundance of the species in catalysis is controlled by the reaction kinetics. Unfortunately, the reaction kinetics is not easily obtained, but it is possible to calculate the equilibrium composition of the system. In equilibrium the distribution of the products will depend on the initial amount of reactants (LiI, $O_2(g)$ and $H_2O(g)$) and the $\Delta G^{o}_{estimate}$ of the reactions. For illustration, we consider a system with a significant excess of LiI (40 mol), limited initial $O_2(g)$ (0 to 3 mol) and either initial $H_2O(g)$ (6 mol) (Figure 5(a)) or no initial $H_2O(g)$ (Figure 5(b)). In addition, only reactions eq 7, 9 and 10 are included. These are the reactions where $\Delta G^{o}_{estimate}$ values are available, but also the reactions that appear to be most favorable based on the reaction energies. The total pressure is kept constant at 0.1 Mpa, and the activity coefficients used in the equilibrium

conditions are approximated by 1. We thereby assume ideal mixing of the different ionic species, i.e., internal energy changes are concentration-independent and entropy of mixing depends only on the individual molar fractions. This is seldom true for ionic mixtures[30] and therefore the equilibrium compositions obtained in these calculations are qualitative. The equilibrium product and reactant distribution is plotted in Figure 5. The first observation is that O_2 is completely consumed at all considered amounts of initial O_2. This is also the case in the experiments (oxygen conversion is 100%). When water is available, LiOH and $I_2(g)$ are the only products formed (Figure 5(a)). Only when gas phase water is absent are Li_2O and a minor amount of $LiIO_4$ formed (Figure 5(b)).

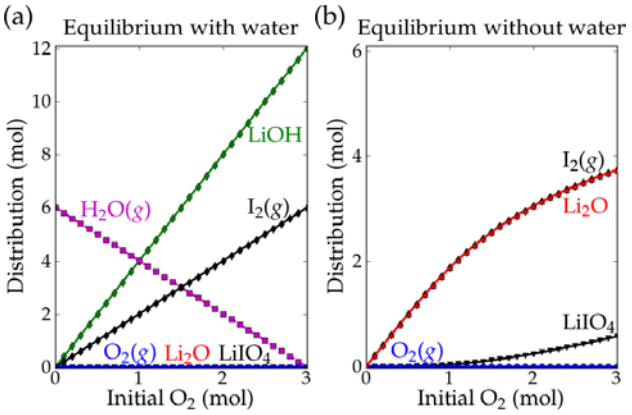

Figure 5. Equilibrium distribution of chemical species. (a) Initial composition of 40 mol LiI, 0 to 3 mol $O_2(g)$ and 6 mol $H_2O(g)$. (b) Initial composition of 40 mol LiI and 0 to 3 mol O_2(g) (no H_2O). Only the reactions of eq 7, 9 and 10 are included. The total pressure is kept constant at standard pressure (0.1 MPa) and the activity coefficients used in the equilibrium equations are approximated by 1.

6. Conclusions

In this study, we have considered the solvation of O_2, H_2O, and I_2 in molten LiI. Solvation of O_2 is associated with an internal energy cost and the degree of molecular solvation is therefore expected to be limited. Solvation of H_2O and I_2 is thermodynamically favorable. In the molten LiI solvent, H_2O coordinates to a Li^+ ion, while I_2 combines with two I^- ions to form I_4^{2-}.

We further considered reactions between O_2, H_2O, and LiI to form the following oxygen-containing species: LiIO, $LiIO_3$, $LiIO_4$, Li_2O_2, Li_2O, and LiOH, where formation of Li_2O_2, Li_2O, and LiOH is accompanied by formation of I_2. It was found that all these reactions are downhill in energy, so reaction kinetics will determine the abundance of the different species.

Unfortunately, the reaction kinetics is not easily accessible. Instead, we evaluated which species will be present if the system is allowed to reach equilibrium. This might not be the case for the actual catalytic system. In the presence of gas phase water, $I_2(g)$ and OH^- are the only species formed. In the absence of water, $I_2(g)$ and O^{2-} will be formed together with a minority of IO_4^-. It is therefore most likely that the ODH activity of molten LiI is due to the formation of solvated and gaseous I_2.

Acknowledgments. Financial support was provided by the Department of Energy, Office of Science, Office of Basic Energy Sciences DE-FG03- 89ER14048 and the Air Force Office of Scientific Research FA9550-12-1-0147. We acknowledge support from the Center for Scientific Computing at the California NanoSystems Institute and the

UCSB Materials Research Laboratory (an NSF MRSEC, DMR-1121053) funded in part by NSF CNS- 0960316 and Hewlett-Packard. Use of the Center for Nanoscale Materials was supported by the U.S. Department of Energy, Office of Science, Office of Basic Energy Sciences, under Contract DE-AC02-06CH11357. Chang Huang would like to acknowledge the China Scholarship Committee for a grant to undertake research at UC Santa Barbara.

Supporting Information Available. Movies showing the molecular dynamics simulations for pure LiI, solvated H_2O, and the formation of I_4^{2-} from solvated I_2 and $2I^-$. This information is available free of charge via the Internet at http://pubs.acs.org.

References

(1) Bartholomew, C. H.; Farrauto, R. J. *Fundamentals of Industrial Catalytic Processes*; Wiley & Sons: Hoboken, NJ, 2006.

(2) Rase, H. F. *Handbook of Commercial Catalysts: Heterogeneous Catalysts*; CRC Press: Boca Raton, 2000.

(3) Lloyd, L. *Handbook of Industrial Catalysis*; Springer: New York, 2011.

(4) Centi, G.; Cavani, F.; Trifiro, F. *Selective Oxidation by Heterogeneous Catalysis*; Kluwer Academic/Plenum Publishers: New York, 2001.

(5) Cavani, F. Catalytic Selective Oxidation: The Forefront in the Challenge for a More Sustainable Chemical Industry. *Catal. Today* **2010,** *157*, 8-15.

(6) Adams, C. T.; Brandenberger, S. G.; DuBois, J. B.; Mill, G. S.; Nager, M.;

Richardson, D. B. Dehydrogenation and Coupling Reactions in the Presence of Iodine and Molten Salt Hydrogen Iodide Acceptors. *J. Organic Chemistry* **1977,** *42*, 1-6.

(7) Nager, M. Dehydrogenation Process. US Patent 3080435, 1963.

(8) Nager, M. Manufacture of Aromatic Hydrocarbons. US Patent 3168584, 1965.

(9) Dahl, I. M.; Grande, K.; Jens, K.-J.; Rytter, E.; Slagtern, Å. Oxidative Dehydrogenation of Propane in Lithium Hydroxide/Lithium Iodide Melts. *Appl. Catal.* **1991,** *77*, 163-174.

(10) Du Bois, J. B. Production of Iodine from Molten Lithium Iodide. US Patent 3169830, 1965.

(11) Kresse, G.; Hafner, J. Ab Initio Molecular Dynamics for Liquid Metals. *Phys. Rev. B* **1993,** *47*, 558-561.

(12) Kresse, G.; Hafner, J. Ab Initio Molecular-Dynamics Simulation of the Liquid-Metal--Amorphous-Semiconductor Transition in Germanium. *Phys. Rev. B* **1994,** *49*, 14251-14269.

(13) Kresse, G.; Furthmüller, J. Efficient Iterative Schemes for Ab Initio Total-Energy Calculations Using a Plane-Wave Basis Set. *Phys. Rev. B* **1996,** *54*, 11169-11186.

(14) Kresse, G.; Furthmüller, J. Efficiency of Ab-Initio Total Energy Calculations for Metals and Semiconductors Using a Plane-Wave Basis Set. *Comput. Mater. Sci.* **1996,** *6*, 15-50.

(15) Perdew, J. P.; Burke, K.; Ernzerhof, M. Generalized Gradient Approximation Made Simple. *Phys. Rev. Lett.* **1996,** *77*, 3865-3868.

(16) Nosé, S. A Unified Formulation of the Constant Temperature Molecular

Dynamics Methods. *J. Chem. Phys.* **1984,** *81*, 511-519.

(17) Yaffe, I. S.; Van Artsdalen, B. R. Electrical Conductance and Density of Pure Molten Alkali Halides. *J. Phys. Chem.* **1956,** *60*, 1125-1131.

(18) Tobias, D. J.; Stern, A. C.; Baer, M. D.; Levin, Y.; Mundy, C. J. Simulation and Theory of Ions at Atmospherically Relevant Aqueous Liquid-Air Interfaces. *Annu. Rev. Phys. Chem.* **2013,** *64*, 339-359.

(19) Levy, H. A.; Agron, P. A.; Bredig, M. A.; Danford, M. D. X-Ray and Neutron Diffraction Studies of Molten Alkali Halides. *Ann. N. Y. Acad. Sci.* **1960,** *79*, 762-780.

(20) Bloom, H. *The Chemistry of Molten Salts*; W. A. Benjamin: New York, 1967.

(21) Kristoffersen, H. H.; Metiu, H. Molten LiCl Layer Supported on MgO: Its Possible Role in Enhancing the Oxidative Dehydrogenation of Ethane. *J. Phys. Chem. C* **2015,** *119*, 8681-8691.

(22) Nangia, P. S.; Benson, S. W. The Kinetics of Dehydrogenation of Propane by Iodine Vapor and the Heat of Formation of the Isopropyl Radical. *J. Am. Chem. Soc.* **1964,** *86*, 2773-2777.

(23) Holleman, A. F.; Wiberg, E. *Inorganic Chemistry*; Academic Press: New York, 2001.

(24) Küpper, F. C.; Feiters, M. C.; Olofsson, B.; Kaiho, T.; Yanagida, S.; Zimmermann, M. B.; Carpenter, L. J.; Luther, G. W.; Lu, Z.; Jonsson, M., et al. Commemorating Two Centuries of Iodine Research: An Interdisciplinary Overview of Current Research. *Angew. Chem. Int. Ed.* **2011,** *50*, 11598-11620.

(25) Awtrey, A. D.; Connick, R. E. The Absorption Spectra of I_2, I_3^-, I^-, IO_3^-, $S_4O_6^-$ and

$S_2O_3^-$. Heat of the Reaction $I_3^- = I_2 + I^-$. *J. Am. Chem. Soc.* **1951,** *73*, 1842-1843.

(26) Stern, K. H. High Temperature Properties and Decomposition of Inorganic Salts, Part 4. Oxy-salts of the Halogens. *J. Phys. Chem. Ref. Data* **1974,** *3*, 481-526.

(27) Evans, T. W.; Dehn, W. M. Organic Oxidations by Iodic Acid. *J. Am. Chem. Soc.* **1930,** *52*, 3647-3649.

(28) Sklarz, B. Organic Chemistry of Periodates. *Quarterly Reviews, Chemical Society* **1967,** *21*, 3-28.

(29) Cota, L. G.; de la Mora, P. On the Structure of Lithium Peroxide, Li_2O_2. *Acta Cryst., Sect. B* **2005,** *61*, 133-136.

(30) Hersh, L. S.; Kleppa, O. J. Enthalpies of Mixing in Some Binary Liquid Halide Mixtures. *J. Chem. Phys.* **1965,** *42*, 1309-1322.

TOC graphic